

**OPTICAL BISTABILITY IN NONLINEAR  
KERR DIELECTRIC  
AND  
FERROELECTRIC MATERIALS**

**by**

**ABDEL-BASET MOHAMED ELNABAWI ABDEL-HAMID IBRAHIM**

**A Thesis submitted to Universiti Sains Malaysia (USM)  
in fulfillment of the requirements for the degree of  
Doctor of Philosophy (Ph.D) in Physics**

**July 2009**

## **ACKNOWLEDGMENTS**

First and foremost I acknowledge my supervisor Professor Junaidah Osman. I thank her for her vision, guidance, involvement, motivation, availability, help and generous support.

I am honored and grateful to Assoc. Prof. Lim Siew Choo for being my co-supervisor, for continuous support, for help with the FRGS grant, and thesis submission. I thank Prof David R. Tilley, Prof Y. Ishibashi, and Dr. Ong Lye Hock for friendly, exciting collaboration, as well as for fruitful suggestions and discussions. I thank Dr. Magdy Hussein for continuous support and for exciting conversation about nonlinear optics.

I thank all the members of my research group, particularly Tan Teng Yong and Ahmad Musleh for creating a friendly, empathic, helpful and stimulating environment. I am deeply indebted to my wife, my parents, and my father in-law for emotional and continuous motivation.

I also acknowledge School of Physics, USM international, and Institute of postgraduate studies (IPS) for friendly environment during various stages of my doctoral studies.

Last but not least I thank the Malaysian Ministry of Higher Education and university sains Malaysia (USM) for financial support for two years under the Fundamental Research Grant Scheme (FRGS) project number 203/PFIZIK/671070.

## TABLE OF CONTENTS

<b>ACKNOWLEDGMENTS</b>	<b>ii</b>
<b>TABLE OF CONTENTS</b>	<b>iii</b>
<b>LIST OF SYMBOLS</b>	<b>viii</b>
<b>ABSTRAK</b>	<b>xiii</b>
<b>ABSTRACT</b>	<b>xvi</b>
<b>CHAPTER 1 GENERAL INTRODUCTION</b>	<b>1</b>
1.1 Motivation of Study	1
1.2 Organization of the thesis	5
<b>CHAPTER 2 FUNDAMENTAL ASPECTS IN NONLINEAR OPTICS</b>	<b>6</b>
2.1 Introduction	6
2.2 Linear Optics of Dielectrics	6
2.2.1 Ionic Crystals	6
2.2.2 Lattice Modes	9
2.2.3 Sources of Polarizability	13
2.2.4 Phenomenological theory for Ionic insulators	17
2.2.5 The Fabry-Pérot resonator	25
2.2.5.1 Theory of Linear Fabry-Perot resonator	26
2.2.5.2 Applications	30
2.3 Nonlinear Optics of Dielectrics	32
2.3.1 Second-Order Processes	34
2.3.1.1 Optical Rectification (OR)	35

2.3.1.2	Second Harmonic Generation (SHG) -----	36
2.3.2	Third-Order Processes -----	37
2.3.2.1	Optical Kerr Effect -----	38
2.3.2.2	Third-Harmonic Generation (THG) -----	39
2.3.3	The Required Input Optical Intensity -----	40
2.3.4	Optical Bistability -----	41
2.3.5	Polarization Optical Bistability and Multistability -----	42
2.3.6	Phase in Optical Communication Systems -----	45
<b>CHAPTER 3</b>	<b>DIELECTRIC OPTICS: OPTICAL BISTABILITY IN KERR NONLINEAR DIELECTRIC MATERIAL BASED ON MAXWELL-DUFFING ANALYSIS -----</b>	<b>48</b>
3.1	Introduction -----	48
3.2	Intrinsic optical bistability (IOB) in nonlinear medium -----	49
3.2.1	Mechanism for Intrinsic Optical Bistability (IOB) -----	49
3.2.2	Physical Origin of Intrinsic Optical Bistability (IOB) -----	51
3.3	Optical Bistability in a Fabry-Perot Resonator -----	52
3.4	Mathematical Formulation -----	55
3.5	Fabry-Perot Analysis -----	61
3.6	Numerical Procedure -----	65
3.7	The Input Parameters -----	67
3.8	Results and Discussion -----	69
3.8.1	Effect of Mirror-----	69
3.8.2	Effect of Angle of Incidence -----	77
3.8.3	Effect of Thickness -----	81
3.9	Conclusion -----	85

<b>CHAPTER 4</b>	<b>GENERAL REVIEW ON FERROELECTRICS</b>	<b>87</b>
4.1	Introduction	87
4.2	Crystal symmetry	89
4.3	Types of Ferroelectrics (FE)	91
4.3.1	Displacive FE	91
4.3.2	Order-Disorder FE	92
4.4	General Properties	93
4.4.1	Dipole Moment	93
4.4.2	Spontaneous Polarization	93
4.4.3	Ferroelectric Domains and Hysteresis Loop	94
4.4.4	Ferroelectric Phase Transitions	98
4.5	Thermodynamic Theory of Ferroelectrics	101
4.6	Ferroelectric Soft-Modes	106
4.6.1	Lyddane-Sachs-Teller (LST) relation	108
4.6.2	The Microscopic Model	111
4.7	Barium Titanate $\text{BaTiO}_3$ (BT)	114
4.8	Optical Applications of Ferroelectrics	121
4.8.1	Applications Related to Intrinsic Optical Properties	122
4.8.1.1	Electro-optic Applications	123
4.8.1.2	Nonlinear Optical Applications	125
4.8.2	Applications Related to Extrinsic Optical Properties	127
4.8.2.1	Waveguides	128
4.8.2.2	Lasers	128
4.8.2.3	Photorefractive applications	129

4.8.2.4	Ferroelectric Structure-Related Applications -----	130
<b>CHAPTER 5 FERROELECTRIC OPTICS: OPTICAL BISTABILITY IN</b>		
<b>KERR FERROELECTRIC MATERIALS ----- 131</b>		
5.1	Introduction-----	131
5.2	Mathematical Formulation -----	133
5.3	Analysis of the Fabry-Perot Interferometer -----	139
5.4	Intrinsic Optical Bistability in Ferroelectrics -----	141
5.5	Material Aspects -----	142
5.6	Numerical Procedure -----	146
5.7	Results and Discussion -----	148
5.7.1	Effect of Mirror Reflectivity -----	148
5.7.2	Effect of Medium Thickness -----	158
5.7.3	Effect of Temperature -----	163
5.7.4	Effect of Frequency -----	169
5.8	Conclusion -----	174
<b>CHAPTER 6 BEHAVIOUR OF DIELECTRIC SUSCEPTIBILITY NEAR</b>		
<b>THE MORPHOTROPIC PHASE BOUNDARY IN</b>		
<b>FERROELECTRIC MATERIALS ----- 177</b>		
6.1	Introduction -----	177
6.2	Background on Morphotropic Phase Boundary (MPB) -----	180
6.3	The Nonlinear Optic Coefficients in Ferroelectric Materials -----	186
6.4	Modeling the MPB Using the Landau-Devonshire Energy -----	193
	Function	
6.5	Results and Discussions -----	196
6.5.1	Linear Dielectric Susceptibility -----	196
6.5.2	Second-Order Nonlinear Susceptibility -----	205

6.5.3	Third-Order Nonlinear Susceptibility -----	216
6.6.	Conclusion -----	229
<b>CHAPTER 7</b>	<b>CONCLUDING REMARKS AND PROSPECTIVE</b>	
	<b>STUDEIES -----</b>	<b>232</b>
<b>REFERENCES</b>	<b>-----</b>	<b>238</b>
<b>APPENDICES</b>		
<b>APPENDIX A</b>	<b>BOUNDARY CONDITIONS BETWEEN TWO</b>	
	<b>MEDIA SEPARATED BY THIN MIRROR -----</b>	<b>252</b>
<b>APPENDIX B</b>	<b>A FLOWCHART DESCRIBING THE</b>	
	<b>NUMERICAL PROCEDURE USED TO OBTAIN THE</b>	
	<b>OPTICAL BISTABILITY CURVES IN CHAPTER 3-----</b>	<b>257</b>
<b>APPENDIX C</b>	<b>A FLOWCHART DESCRIBING THE</b>	
	<b>NUMERICAL PROCEDURE USED TO OBTAIN THE</b>	
	<b>OPTICAL BISTABILITY CURVES IN CHAPTER 5-----</b>	<b>258</b>
<b>LIST OF PUBLICATIONS</b>	<b>-----</b>	<b>259</b>

## LIST OF SYMBOLS

Symbol	Definition
$\alpha$	Nonlinear coefficient of the second-order term in the free energy
$\mathbf{a}$	Total polarizability
$\beta$	Nonlinear coefficient of the fourth-order term in the isotropic free energy
$\beta_1$	Nonlinear coefficient of the fourth-order pure term in anisotropic free energy
$\beta_2$	Nonlinear coefficient of the fourth-order cross term in the anisotropic free energy
$\gamma$	Coupling coefficient
$\Gamma$	Damping parameter
$\delta_M$	Mirror thickness
$\Delta$	The difference between the squared resonance frequency and the squared operating frequency
$\Delta_s$	The scaled form of $\Delta$
$\varepsilon(\omega)$	The frequency-dependent linear dielectric function
$\varepsilon_s$	static dielectric constant
$\varepsilon_0$	Dielectric permittivity of free space
$\varepsilon_\infty$	The high-frequency limit of the linear dielectric function
$\varepsilon_M$	Dielectric permittivity of the mirror medium.
$\eta$	Complex mirror coefficient
$\eta_s$	Scaled complex mirror coefficient
$\eta_{s,r}$	Real part of the scaled mirror coefficient

$\eta_{s,i}$	Imaginary part of the scaled mirror coefficient
$\Theta_i$	Angle of incidence
$\Theta_r$	Angle of reflectance
$\Theta_2$	Angle of refraction
$\Theta_t$	Exit angle
$\mu_0$	Magnetic permeability of free space
$\nu$	Nonlinear coefficient for the sixth-order term in the isotropic free energy
$\rho$	Elementary (Fresnel) reflection coefficient
$\sigma(n\omega)$	Linear response function of ferroelectric material
$\sigma_M$	Conductivity of mirror medium
$\tau$	Complex transmission coefficient
$\phi$	Phase function
$\chi$	Dielectric susceptibility
$\omega$	Operating frequency of the driving field
$\omega_0$	Resonance frequency of the material
$\omega_T$	Transverse-optical phonon frequency
$\omega_L$	Longitudinal-optical phonon frequency
$\omega_p$	Plasma frequency of the material
$a$	Inverse of the Curie constant
$b$	Nonlinear coefficient in Duffing anharmonic equation

$c$	Velocity of light
$C$	Curie constant
$d$	Second-order nonlinear coefficient corresponds to second-order susceptibility $\chi^{(2)}$ .
$e_0$	Scaled electric field amplitude in free space (Vacuum)
$E_0$	Dimensional Electric field amplitude in free space (Vacuum)
$E_c$	Coercive field of ferroelectric material
$e$	Scaled electric field in a medium
$\mathbf{E}$	Dimensional Time-dependent electric
$E$	Dimensional Time-independent electric field
$f$	Scaled operating frequency
$F$	Free energy of ferroelectrics
$g$	Scaled damping parameter of dielectric medium
$g_F$	Scaled damping parameter of ferroelectric medium
$G$	Order parameter in Taylor expansion
$\mathbf{H}$	Time-dependent magnetic field
$k_0$	Wavenumber in free space
$k_{2y}$	y-component of the wavenumber
$\hat{\kappa}$	Extinction coefficient
$k_{2z}$	z-component of the wavenumber
$K$	Wavenumber

$\mathcal{K}$	Wavevector in arbitrary direction
$l$	Scaled thickness
$L$	Thickness of the nonlinear medium
$m$	Scaled reduced mass per unit cell
$M$	Dimensional Reduced mass per unit cell
$n_2$	Effective refractive index in medium 2
$n_{2T}$	Transverse refractive index in medium 2
$N$	Number density of ions
$p$	Dipole moment or microscopic polarization
$p$	Scaled macroscopic polarization amplitude
$P$	Macroscopic polarization amplitude
$P_s$	Spontaneous polarization in ferroelectrics
$\mathbf{P}$	Macroscopic time-dependent polarization
$q$	Effective charge per ion
$Q$	Polarization of ferroelectric material in tetragonal phase
$r$	Complex reflection coefficient
$\mathbf{R}$	Reflectance or reflectivity of the nonlinear medium
$R_M$	Reflectivity of the mirror medium
$s(n\omega)$	Linear response function of ferroelectric material corresponds to linear dielectric susceptibility element $\chi_{zz}(n\omega)$
$t$	Scaled thermodynamic temperature of ferroelectric material
$\mathbf{t}$	Time
$T$	Thermodynamic temperature of ferroelectric material

$T_c$	Curie temperature
<b>T</b>	Transmittance of a medium
$u$	Scaled distance in $z$ -direction
$w$	Scaled plasma frequency
$x$	Displacement of ions from its equilibrium position
$y$	Displacement along $y$ -direction in $xyz$ Cartesian coordinate system
$z$	Displacement along $z$ -direction in $xyz$ Cartesian coordinate system

# **DWI-KESTABILAN OPTIK DI DALAM BAHAN-BAHAN DIELEKTRIK TAK LINEAR KERR DAN FEROELEKTRIK.**

## **ABSTRAK**

Kestabilan optiks dwi dan kestabilan optiks pelbagai di dalam hablur Kerr tak linear dikaji. Dua jenis sistem hablur penebat berion dipertimbangkan: bahan dielektrik biasa dan bahan ferroelektrik (FE) dengan struktur Perovskit. Kedua-dua ketakstabilan optiks ekstrinsik dan instrinsik dikaji. Suatu analisis alternatif digunakan untuk memodelkan kestabilan optiks tersebut; berbanding dengan analisis lazim di mana pengkutuban tak linear biasanya dikembangkan sebagai siri Taylor dalam medan elektrik. Formalisma alternatif ini terbukti lebih sesuai untuk bahan tak linear yang tinggi seperti FE dan bagi ketaklinearan resonan. Kestabilan optiks ini terselah pada beberapa pembolehubah-pembolehubah fizikal seperti pengkutuban, pekali-pekali pantulan dan biasan. Kesan-kesan oleh ketebalan sistem, frekuensi operasi, parameter lembapan, dan pekali ketaklinearan ke atas kestabilan optiks bagi setiap sistem hablur dikaji.

Persamaan Duffing yang menerangkan pengayun tak harmonik dan persamaan gelombang digunakan untuk memodelkan respons tak linear sistem dielektrik. Aplikasi syarat-syarat sempadan lazim memberikan rumus analitik bagi pekali-pekali pantulan dan biasan yang diungkap dalam sebutan amplitud medan tuju elektrik, pengkutuban dan parameter-parameter bahan yang lain. Keputusan-

keputusan simulasi bernombor menunjukkan bahawa kestabilan optiks sistem bergantung kepada ketebalan bahan, pekali ketaklinearan, dan sudut tuju setiap sistem hablur. Bagi kes alat resonan dielektik Fabry-Pérot, kestabilan optikisnya didapati bergantung kepada kepantulan cermin.

Bagi sistem FE, respons tak linearnya dimodelkan dengan menggunakan persamaan dinamik Landau-Khalatnikov (LK). Keupayaan tak harmonik tak linearnya diperolehi dari tenaga bebas Landau-Devonshire (LD) yang telah diungkap dalam sebutan pengkutuban sistem. Dengan menggunakan penghampiran frekuensi tunggal, persamaan LK dan persamaan gelombang digunakan untuk menghasilkan persamaan pengkutuban tak linear. Teknik ini membuatkan kestabilan optiks sistem menjadi bergantung kepada suhu. Ungkapan analitik bagi kedua-dua pekali pantulan dan biasan sebagai fungsi suhu dan parameter-parameter bahan yang lain diterbitkan. Parameter-parameter input diperolehi dari data eksperimen yang sedia ada bagi hablur tunggal  $\text{BaTiO}_3$  untuk digunakan di dalam simulasi bernombor. Keputusan-keputusan simulasi bersetuju pada prinsipnya dengan pemerhatian eksperimen ke atas kestabilan optiks intrinsik di dalam hablur mono  $\text{BaTiO}_3$  dan di dalam bahan-bahan fotorefraktif FE. Didapati bahan-bahan FE ini sentiasa mempamerkan kestabilan jenis 'threshold'.

Bahagian terakhir kerja penyelidikan ini tertumpu kepada kajian kerentanan dielektrik bagi bahan pukal FE berhampiran sempadan fasa morfotropik (MPB). Ini termasuk kajian ke atas kerentanan linear dan taklinear (peringkat kedua dan ketiga) bagi kedua-dua had dinamik dan statik. Tabii kerentanan-kerentanan ini dikaji berhampiran MPB dengan menggunakan tenaga bebas LD dan persamaan dinamik LK. Magnitud kerentanan-kerentanan dilakar sebagai fungsi bahan parameter

$\beta^* = \beta_2/\beta_1$  di mana  $\beta_1$  and  $\beta_2$  adalah pekali-pekali di dalam ungkapan tenaga bebas LD. Dalam had statik, MPB diwakilkan oleh nilai  $\beta^* = 1$ . Dalam had ini, pemalar dielektrik linear adalah malar, kerentanan-kerentanan tak linear peringkat kedua dan ketiga mencapah di MPB. Kerentanan dielektrik dinamik didapati mempunyai puncak atau puncak-puncak pada sesuatu nilai/nilai-nilai  $\beta^*$ . Pertambahan ini boleh difahami dengan menggunakan konsep frekuensi normal  $\omega_T$  dalam mod lembut FE. Pertambahan dalam nilai kerentanan tak linear ini mempunyai potensi di dalam menjuruterakan bahan baru untuk applikasi beberapa peranti-peranti optiks.

# **OPTICAL BISTABILITY IN NONLINEAR KERR DIELECTRIC AND FERROELECTRIC MATERIALS**

## **ABSTRACT**

The optical bistability (OB) and multistability in Kerr nonlinear crystals are investigated. Two types of ionic insulating crystals are considered: a typical dielectric and a ferroelectric (FE). Both extrinsic and intrinsic optical instabilities are investigated. An alternative analysis is used to model the OB; rather than the conventional analysis where the nonlinear polarization is usually expanded as the Taylor series in the electric field. The alternative formalism proves to be more suitable for highly nonlinear materials such as FE and for resonant-nonlinearities. The OB has its manifestation in various physical variables such as polarization, reflectance and transmittance coefficients. The effects of system thickness, operating frequency, damping parameter, and nonlinearity coefficient, on the OB of each crystal system are investigated.

The Duffing equation describing an anharmonic oscillator and the wave equation are used to model the nonlinear response of the material. Application of standard boundary conditions leads to analytical expressions for both reflectance and transmittance expressed in terms of the electric field incident amplitude, polarization and other material parameters. Numerical simulations show that the OB is dependent on the material thickness, nonlinear coefficient, and the angle of incidence. In the case of a dielectric Fabry-Pérot resonator, the OB is also found to be mirror reflectivity dependent.

For FE material, the nonlinear response is modeled using the Landau-Khalatnikov (LK) dynamical equation. The nonlinear anharmonic potential is obtained from the Landau-Devonshire (LD) free energy expressed in terms of polarization. The LK equation and the wave equation are then used to produce a nonlinear polarization equation. This technique makes the OB becomes temperature-dependent. Input parameters from available experimental data of a BaTiO<sub>3</sub> single crystal are used in the numerical simulations. The simulation results agree in principle with the recent experimental observations of intrinsic OB in BaTiO<sub>3</sub> monocrystal and other FE photorefractive materials. It is found that FE always exhibits a threshold-type of bistability.

The last part of this work is devoted to studies of dielectric susceptibilities of bulk FE materials in the vicinity of the morphotropic phase boundary (MPB). It includes studies on linear and nonlinear (second-order and third-order) susceptibilities for both the dynamic and static limit. The behaviour of the susceptibilities near the MPB is investigated using the LD free energy and LK dynamical equation. The susceptibility magnitudes are plotted as a function of the material parameter  $\beta^* = \beta_2/\beta_1$  where  $\beta_1$  and  $\beta_2$  are the coefficients in the LD free energy expression. In the static limit, the MPB is represented by  $\beta^* = 1$ . In this limit, the linear dielectric constant, the second third-order nonlinear susceptibilities diverge at the MPB. The dynamic dielectric susceptibility assumes a resonance-like peak(s) or peaks at certain value(s) of  $\beta^*$ . The enhancement is explained using the concept of FE soft-mode. The enhancement of the nonlinear susceptibility may have its potential in engineering new materials for various optical device applications.

# Chapter 1

## GENERAL INTRODUCTION

### 1.1 Motivation of Study

Optical technology is employed in CD-ROM drives and their relatives, laser printers, and most photocopiers and scanners. However, none of these devices are fully optical; all rely to some extent on conventional electronic circuits and components. Optical technology has made its most significant inroads in digital communications, where fiber optic data transmission has become commonplace. The ultimate goal is the so-called photonic network, which uses visible and IR energy exclusively between each source and destination.

The current communication network operates based on a combination of both electronics and photonics (hybrid). It consists of nodes which are connected by a series of fiber-optic links. These fiber-optic links are used to transmit the information while the nodes decide which path the information should follow from source to destination (routing). While the fiber-optic links carry the information via light, the nodes are still mostly electrical. In the past, this hybrid technology has served the data-communication networks adequately. At present, this technology is predicted to breakdown as the demand for telecommunication services is increasing exponentially. The rapid growth of the Internet, expanding at almost 15% per month, demands faster speeds and larger bandwidths than electronic circuits can provide. Electronic switching limits network speeds to about 50 Gigabits per second (1 Gigabit is  $10^9$  bits).

Fortunately, for long distance communications, a very high capacity dispersion-free transmission can be realized either by implementing solitons and other types of nonlinear pulse transmission in optical fiber. However, it seems that the bottlenecks are the data processing and switching components in the nodes. Therefore, the aim is to replace the nodes based on electrical technology by optical ones. As such, the study of optical phenomena in nonlinear waveguides (optical bistability) has been intensified, in the hope that these can be used for all-optical switching purposes.

On the other hand, there has been intensive research for developing an optical computer that might operate 1000 times faster than an electronic computer (Abraham 1983, and, Brenner 1986). An optical computer is a computer that performs its digital computation with photons in visible light or infrared as opposed to the more traditional electron-based computation (silicon technology). The electronic computer have its fundament limit since an electric current flows at only about 10 percent of the speed of light which limits the rate at which data can be exchanged over long distances. The fundamental components of any digital computer are; memory, processor, and terminals for information. The three basic functions of a computer are arithmetic operation, logical operations and the memory. All these functions are done by devices that have bistable states (true and false). In arithmetic operation the two states represent the numbers 0 and 1 of the binary number system. The memory of the computer also stores the results of arithmetic and logical operation in bistable devices. Thus a computer requires an optical transistor that can represent the values 0 and 1 in physical form. Moreover, optical transistors can be assembled into larger scale devices that perform the three logical functions: AND, OR and NOT.

Optical switching is a natural candidate to mediate between electronic systems and optical ones. The starting point of the optical transistor is an ingenious and widely used optical apparatus known as the Fabry-Perot interferometer. When the Fabry-Perot apparatus is filled with an intensity-dependent nonlinear medium, and a powerful source of coherent radiation is focused, the transmitted intensity assumes a bistable state when the input laser is varied. Therefore, optical switches can be made in the form of thin nonlinear crystals. Current techniques of crystal growing or thin-film fabrication make it possible to fabricate very large thin sheets. If an optical image was projected directly through a large sheet in which each small area served as an optical switch, the transmission from the switches would serve as a digital record of the image. Many kinds of processing and enhancement of the image could be done while the record was being made.

In addition to the above, optical devices have an inherent capability for parallel processing since every pixel of a two-dimensional image can be both relayed and processed at the same time. This parallelism capability when associated with fast switching speeds would result in staggering computational power. For example, a calculation that might take a conventional electronic computer more than eleven years to complete could be performed by an optical computer in a single hour. It is also justified to consider applying the new optical information processing techniques for protecting data and biometrics against tampering (Javidi 1997). Information can be hidden in any of several dimensions such as the phase, wavelength, spatial frequency or polarization of the light.

In order to design such bistable devices, it is extremely important to understand the physical phenomena appearing in the structures. To predict the behaviour of light in

the structures; analytical descriptions or at least numerical simulations are essential. A major part of this thesis is devoted to the study of optical bistability in a Fabry-Perot interferometer filled with an intensity-dependent Kerr nonlinearity. The intrinsic optical bistability results from a Kerr nonlinear film made of an insulating ionic crystal is also investigated. The optical bistability is investigated for both dielectric and ferroelectric materials. It is hoped that this work might help to contribute towards the understanding of optical bistability in a nonlinear materials in a hope that optical switches and eventually optical computers and all-optical digital networks become possible.

For these all-optical devices to be implemented, it would be highly beneficial to search for highly-nonlinear optical materials. One way is to engineer a specific nonlinear material through the concept of morphotropic phase boundary (MPB) at which the dielectric and mechanical properties of the material is maximum. The MPB knowledge can be used as one of the general guiding principles in the search for materials with large NL dielectric susceptibility coefficients. Particularly, the MPB work presented here may stimulate further interest in the fundamental theory of nonlinear response of single ferroelectric crystals with simple structure such as  $\text{BaTiO}_3$  or  $\text{PbTiO}_3$ . Such pure materials can be used for technological applications rather than material with complicated structure which require a complicated and costly process to process its solid solutions as well as introducing complexity in the study of the microscopic origins of their properties.

## **1.2 Organization of the Thesis**

This thesis consists of seven chapters. Chapter 2 gives some general review on certain aspects of linear and nonlinear optics of dielectrics with emphasis on topics

directly related to this study. Chapter 3 contains an investigation on the optical bistability in a Fabry-Pérot resonator filled with a nonlinear Kerr dielectric material using the Maxwell-Duffing analysis. In this chapter we give a detailed analysis of optical bistability manifested through polarization and phase. We also differentiate between two distinct types of bistable behaviour, namely extrinsic and intrinsic optical bistability, and explain the physics behind each type. Chapter 4 gives a review on ferroelectric properties directly related to this study. This includes the basic concept of spontaneous polarization, hysteresis loop, the Landau-Devonshire theory of phase transitions, and ferroelectric soft modes. Finally, the application of ferroelectric materials is also presented. Chapter 5 presents the Maxwell-Duffing analysis to investigate the optical bistability in Kerr material ferroelectric materials. Particularly a ferroelectric Fabry-Pérot resonator and a ferroelectric film are considered. Here the thermodynamic free energy is used with the Landau-Khalatnikov equation to develop a semi-analytical analysis suitable for ferroelectric materials. In chapter 6, we present the study on the behavior of the second and third-order nonlinear susceptibilities in the vicinity of the morphotropic phase boundary (MPB) in ferroelectrics. Here, the origin of the large values of the NL susceptibility tensor components at the MPB is investigated. The enhancement of the dynamic nonlinear susceptibility tensors is investigated within the concept of the ferroelectric soft-mode. The enhancement of various elements of particular NLO process such as second-harmonic generation (SHG), optical rectification (OR), third-harmonic generation (THG), and intensity-dependent refractive index (IP) is investigated at the MPB. In Chapter 7 we conclude the results of this study and suggest some possible areas for future work.

## **Chapter 2**

### **FUNDAMENTAL ASPECTS IN LINEAR AND NONLINEAR PROPERTIES OF DIELECTRIC MATERIALS**

#### **2.1 Introduction**

This aim of this chapter is to provide some general review on the field of linear and nonlinear properties of dielectric materials related to this study. In the first section we review certain aspects in linear optics of dielectrics with emphasizing on some relevant condensed matter theories needed to understand this work. Particularly, we introduce some basic information about ionic crystals, lattice modes, sources of polarizability, phenomenological theory of ionic crystals, and the linear Fabry Péroter interferometer.

In the second-section we review certain aspects in nonlinear optics directly related to our work. More specifically, in the second-order nonlinear optics, we review the optical rectification (OR), and the second harmonic generation (SHG). In the third-order nonlinear optics, we review the optical Kerr effect, and the third harmonic generation (THG). Further, we review certain nonlinear optical phenomenon related to optical Kerr-effect such as polarization and phase optical bistability

#### **2.2 Linear Optics of Dielectrics**

##### **2.2.1 Ionic Crystals**

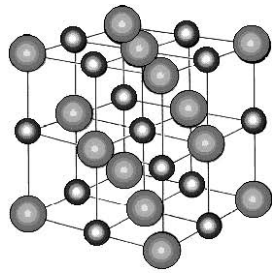
Crystals are classified according to their physical and chemical properties to ionic, covalent, metallic, or molecular. Ionic and molecular crystals are usually dielectrics

while covalent crystal may be dielectric or semiconductors. The type of chemical bond has its manifestation in the optical properties. For example, ionic and covalent crystals are transparent or absorbing in the infrared region while metals are opaque and reflect light well. We are mainly concerned here with the ionic type of crystals because of its importance in the field of nonlinear optics. Being readily available and among the simplest known solids, ionic crystals have been a frequent and profitable meeting place between theory and experiment. This is in contrast to metals and covalent crystals, which are bound by more complicated forces, and to molecular crystals, which either have complicated structures or difficult to produce as single crystals.

In ionic crystals, the lattice-site occupants are charged ions held together primarily by their electrostatic interaction. Such binding is called ionic binding. For example, in a compound  $(A)_n(B)_m$  we can expect ionic bonding to predominate when atom A has a strong electropositivity and atom B has a strong electronegativity. In this case electron transfer from one atom to another leads to the formation of  $A^+B^-$ . For the main group elements the electron transfer continues until the ions have closed shell configurations. Therefore, ionic crystals can be described as an ensemble of hard spheres which try to occupy a minimum volume while minimizing electrostatic energy at the same time. Empirically, ionic crystals are distinguished by strong absorption of infrared radiation and the existence of planes along which the crystals cleave easily (Maier 2004). Most ionic crystals have large band gaps, and are therefore generally electronic insulators. In perfect lattice where all lattice sites are fully occupied, ions cannot be mobile. However, electrical conduction may occur via the motion of ions through these crystals due to high temperature or due to the presence of point defects.

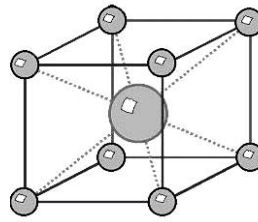
Ionic crystals have at least two atoms in their base which are ionized. Charge neutrality demands that the total charge in the base must be zero. Examples of ionic crystals are alkali halides, monovalent metal halides, alkaline-earth halides, oxides, and sulfides. The ideal ionic crystal is approached most closely by the alkali halides which have a simple chemical formula  $XY$ , where  $X$  is an alkali metal and  $Y$  is a halogen (Sirdeshmukh 2001). One of the most well known of these is sodium chloride ( $\text{NaCl}$ ). Ionic crystals, especially alkali halides, are relatively easy to produce as large, quite pure, single crystals suitable for accurate and reproducible experimental investigations. In addition, they are relatively easy to subject to theoretical treatment since they have simple structures and are bound by the well-understood Coulomb force between the ions.

Ionic crystals come in simple and more complicated lattice types (Rao 1997). Some prominent lattice types of ionic crystals include the “ $\text{NaCl}$  Structure” where the lattice is face-centered cubic (fcc) with two atoms in the base: one at  $(0,0,0)$ , the other one at  $(1/2,0,0)$ . Many salts and oxides have this structure such as  $\text{KCl}$ ,  $\text{MgO}$  or  $\text{FeO}$ . The second lattice type is “perovskite structure” with cubic-primitive lattice, but may be distorted to different symmetry. It is also known as the  $\text{BaTiO}_3$  or  $\text{CaTiO}_3$  lattice and has three different atoms in the base. For  $\text{BaTiO}_3$ , it would be  $\text{Ba}$  at  $(0,0,0)$ ,  $\text{O}$  at  $(1/2,1/2,0)$  and  $\text{Ti}$  at  $(1/2,1/2,1/2)$ . Other lattice types include the “ $\text{CsCl}$  Structure” and the “ $\text{ZnS}$  Structure”, and the  $\text{ZrO}_2$  as shown in Fig. 2.1.



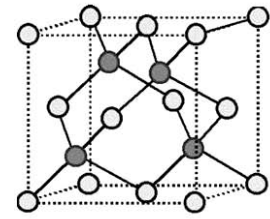
**The NaCl Structure**

(a)



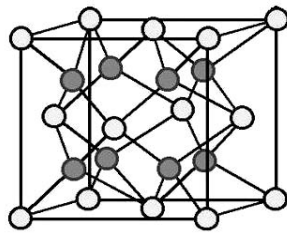
**The CsCl Structure**

(b)



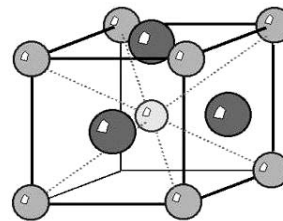
**The ZnS Structure**

(c)



**The ZrO<sub>2</sub> Structure**

(d)



**The Perovskite Structure**

(e)

**Figure 2.1 Some prominent lattice types of ionic crystals**

### 2.2.2 Lattice Modes

A crystal lattice at zero temperature lies in its ground state, and contains no phonons. According to thermodynamics, when the lattice is held at a non-zero temperature its energy is not constant, but fluctuates randomly about some mean value. These energy fluctuations are caused by random lattice vibrations. The atoms vibrate as a linear chain independent of the number of different atoms per lattice cell. Due to the connections between atoms, the displacement of one or more atoms from their equilibrium positions will give rise to a set of vibration waves propagating through the lattice. The amplitude of the wave is given by the displacements of the atoms from their equilibrium positions. A phonon is a quantized mode of vibration

occurring in a rigid crystal lattice, such as the atomic lattice of a solid (Kittel 1995). Because these phonons are generated by the temperature of the lattice, they are sometimes referred to as “thermal phonons”.

In solids with more than one atom in the smallest unit cell (non-primitive unit cell), there are two types of phonons: "acoustic" and "optical". A schematic diagram for both acoustic and optical phonons is shown in Fig. 2.2(a). Acoustic phonons correspond to a mode of vibration where positive and negative ions in a primitive unit cell vibrate together in phase (Ashcroft 1976). Acoustic phonons have frequencies that become small at the long wavelengths, and correspond to sound waves in the lattice. Therefore, it does not couple with electromagnetic waves. For each atom in the unit cell, one expects to find three branches of phonons (two transverse, and one longitudinal). A solid that has  $N$  atoms in its unit cell will have  $3(N-1)$  optical modes. And again, each optical mode will be separated into two transverse branches and one longitudinal branch (Waser 2005).

Optical phonons always have some minimum frequency of vibration, even when their wavelength is large. They are called "optical" because in ionic crystals, they are excited very easily by light or infrared radiation. This is because they correspond to a mode of vibration where positive and negative ions in a unit cell vibrate against each other (out of phase) leaving the center of mass at rest as shown in Fig. 2.2(b). Thus, they create a time-varying electrical dipole moment which allow coupling to the electromagnetic waves either by absorbing or scattering. Optical phonons that interact in this way with light are called infrared active. Optical phonons are often abbreviated as LO and TO phonons, for the longitudinal and transverse varieties respectively. A vibration of the atoms perpendicular to the propagation corresponds

to a TO wave while a vibration in the direction of the propagation corresponds to an LO wave. The dispersion relation between the frequency of the mode  $\omega$  and its wave vector  $k$  have two branches Fig. 2.2(a), the first branch is the TA mode with frequency vanishes linearly with wavevector, and the other branch is the TO mode where the frequency has a finite value at  $k = 0$ .

In general, each mode of the phonon dispersion spectra is collectively characterized by the relating energy, i.e. the frequency and wave vector  $k$ , and is associated with a specific distortion of the structure. The local electric field in ionic crystals leads to a splitting of the optical vibration modes. The LO mode frequency is shifted to higher frequencies while the TO mode frequency is shifted to lower frequencies. The softening of the TO modes is caused by a partial compensation of the short-range lattice (elastic) forces on one hand and the long-range electric fields on the other hand.

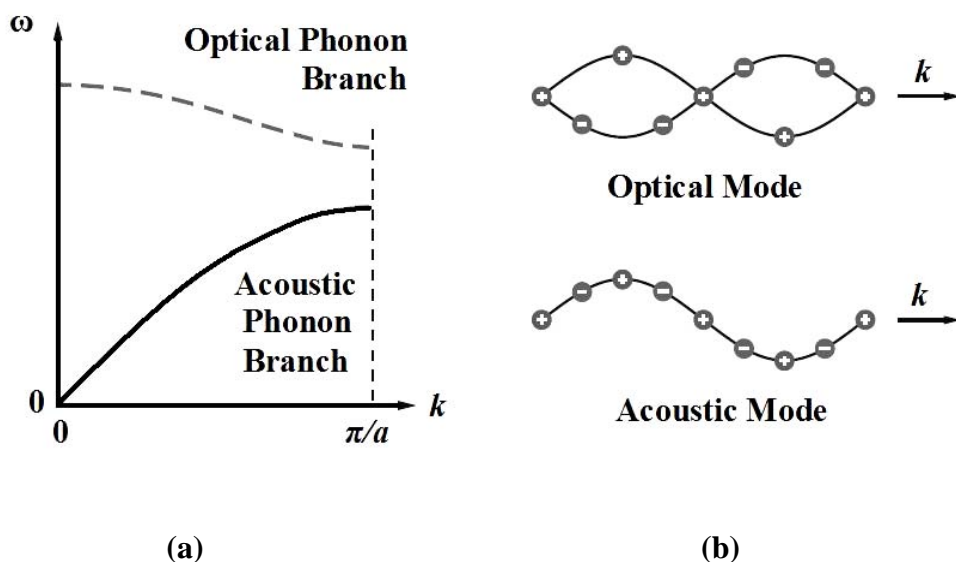


**Figure 2.2** (a) Transverse acoustic (TA) and optic mode (TO) of the phonon spectrum. (b) a pattern of atomic displacements for an acoustic and an optical phonon mode of the same wave vector (Waser 2005).

If the compensation is complete, the TO-mode frequency becomes zero when the temperature approaches  $T_c$ ,  $\omega_{TO}(T \rightarrow T_c) \rightarrow 0$ , and the soft phonon condenses out so that at  $T_c$  a phase transition to a state with spontaneous polarization takes place (ferroelectric phase transition). At the zone center  $k \rightarrow 0$ , the wavelength of the TO mode is infinite  $\lambda \rightarrow \infty$ . In this case the optical modes have highest energy where the two sublattices move rigidly against each other Fig. 2.2(c). In this case, the dispersion curve is nearly constant and assumes its maximum and the optical modes couple strongly to the electromagnetic field. In the case of the softening of the TO mode, the transverse frequency becomes zero and no vibration exists anymore “frozen in” (Waser 2005). The relation between  $\omega_{TO}^2$  and  $T$  at the zone center is found to be linear as shown in Fig. 2.2(d) suggesting the temperature dependence of the optic mode frequency relates to the phase transitions.

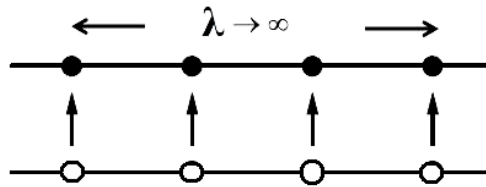


**Figure 2.2(c) freezing of the TO modes for  $T \rightarrow T_c$  (Waser 2005).**

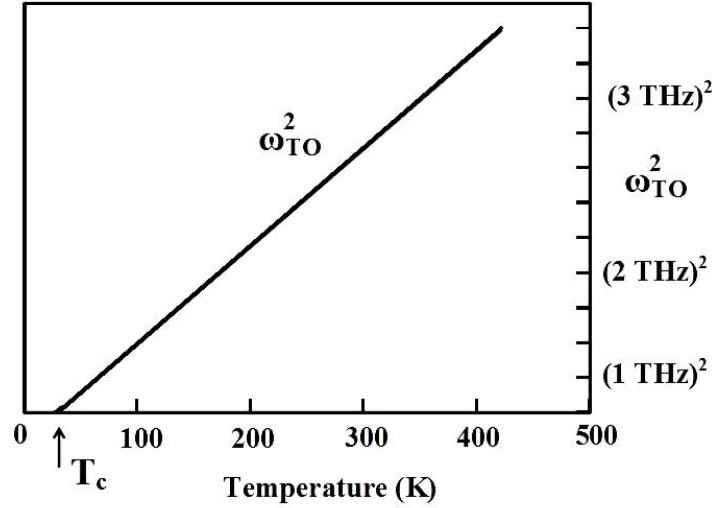


**Figure 2.2(d) Frequency of the TO mode and dielectric behavior at the phase transition**

### 2.2.3 Sources of Polarizability

The constitutive equation that includes the response of the material to the applied electromagnetic field is written as;

$$\vec{D} = \epsilon_0 \vec{E} + \vec{P} \quad (2.1)$$

where  $\vec{D}$  is the electric displacement. The term  $\epsilon_0 \vec{E}$  represents the vacuum contribution caused by the externally applied electric field and  $\vec{P}$  is the electrical polarization of the matter. This relation is independent of the nature of the polarization which could pyroelectric, piezoelectric or dielectric polarization. The macroscopic polarization created by the dipoles adds to the vacuum contribution and sums up to the displacement field  $\vec{D}$ . For different frequencies, different types of oscillators will dominate the response. The strength of this response depends also on the oscillator density and on the inertia of the excitation mechanism. For a pure

dielectric response, the polarization is proportional to the electric field in a linear approximation by

$$\vec{P} = \varepsilon_0 \chi \vec{E} \quad \text{or} \quad \vec{D} = \varepsilon_0 \varepsilon_r \vec{E} \quad (2.2)$$

Equations. (2.1)-(2.2) describe the mean properties of the dielectric. The dielectric susceptibility  $\chi$  is related to the relative dielectric constant  $\varepsilon_r$  by  $\chi = \varepsilon_r - 1$ . Equations (2.2) are only valid for small fields. Large amplitudes of the ac field lead to strong nonlinearities in dielectrics, and hysteresis loops in ferroelectrics. This macroscopic point of view does not consider the microscopic origin of the polarization (Kittel 1995). The macroscopic polarization  $\mathbf{P}$  is the sum of all the individual dipole moments  $\mathbf{p}_j$  of the material with the density  $N_j$ .

$$\mathbf{P} = \sum_j N_j \mathbf{p}_j \quad (2.3)$$

In order to find a correlation between the macroscopic polarization and the microscopic properties of the material, a single (polarizable) particle is considered. A dipole moment is induced by the electric field at the position of the particle which is called the local electric field  $\mathbf{E}_{loc}$

$$\mathbf{P} = \alpha \mathbf{E}_{loc} \quad (2.4)$$

where  $\alpha$  is the polarizability of an atomic dipole. If there is no interaction between the polarized particles, the local electric field is identical to the externally applied electric field  $\mathbf{E}_{loc} = \mathbf{E}_0$ . The local field  $\mathbf{E}_{loc}$  at the position of a particular dipole is given by the superposition of the applied macroscopic field  $\mathbf{E}_0$  and the sum of all other dipole fields. In general, there are five different mechanisms of polarization which can contribute to the dielectric response (Kittel 1995).

- **Electronic polarization** exists in all dielectrics. It is based on the displacement of the negatively charged electron shell against the positively charged core. The electronic polarizability is approximately proportional to the volume of the electron shell. Thus, in general electronic polarization is temperature-independent, and large atoms have a large electronic polarizability.
- **Ionic polarization** is observed in ionic crystals and describes the displacement of the positive and negative sublattices under an applied electric field.
- **Dipolar polarization** describes the alignment of permanent dipoles. At ambient temperatures, usually all dipole moments have statistical distribution of their directions. An electric field generates a preferred direction for the dipoles, while the thermal movement of the atoms perturbs the alignment.
- **Space charge polarizability** is caused by a drift of mobile ions or electrons which are confined to outer or inner interfaces. It can exist in dielectric materials which show spatial inhomogeneities of charge carrier densities. Its effects are not only important in semiconductor field-effect devices, but also in ceramics with electrically conducting grains and insulating grain boundaries as well. Depending on the local conductivity, the space charge polarization may occur over a wide frequency range from mHz up to MHz and is temperature-independent.
- **Domain wall polarization** exists in ferroelectric materials and contributes to the overall dielectric response. The motion of a domain wall that separates regions of different oriented polarization takes place by the fact that favored oriented domains with respect to the applied field tends to grow.

The total polarizability  $\alpha$  of dielectric material results from all the contributions discussed above. The contributions from the lattice are called intrinsic contributions, in contrast to extrinsic contributions.

$$\alpha = \underbrace{\alpha_e + \alpha_i}_{\text{intrinsic}} + \underbrace{\alpha_{dip} + \alpha_{domain} + \alpha_{space\ charge}}_{\text{extrinsic}} \quad (2.5)$$

If the oscillating masses experience a restoring force, a relaxation behavior is found (for orientation, domain walls, and space charge polarization). Resonance effects are observed for both ionic and electronic polarization. In the infrared region between 1 and 10 THz, resonances of the molecular vibrations and ionic lattices constituting the upper frequency limit of the ionic polarization are observed.

Fig. 2.3 presents a schematic picture of different polarization mechanisms that occur in solid materials. The figure shows that for different frequencies, different oscillators are excited. In these frequency intervals, close to the oscillator resonances, the polarizability of the material varies strongly with frequency. For frequencies between the resonances the polarizability is almost constant. It is characteristic for an oscillator that there is a resonance region with strong absorption and dispersion. A resonance located at a high frequency will give frequency-independent contribution at all lower frequencies, whilst a low frequency resonance will not contribute at sufficiently high frequencies due to inertia.

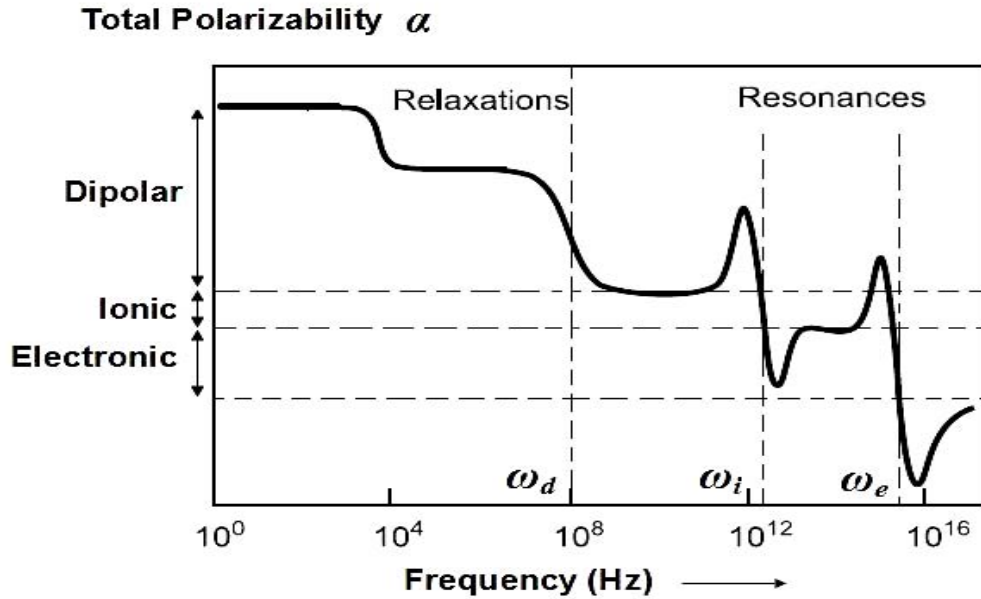


Figure 2.3 Total polarizability (real part) versus frequency for dipolar substance. The parts of the spectrum where the resonances are located are indicated.  $\omega_e$ ,  $\omega_i$ , and  $\omega_d$  are resonances of the electronic polarization, ionic polarization, and dipolar polarization respectively.

#### 2.2.4 Phenomenological theory for Ionic insulators

when an electric field interacts with a nonlinear medium, the material is thought of as a collection of charged particles (electrons and ions). Upon applying the electric field, the positive charges tend to move in the direction of the field while the negative one move the opposite way. In dielectric material, the charged particles are bounded together yet the bond has certain elasticity. The slight displacement of the positive and negative charges from their equilibrium positions results in an induced electric dipole moments. Because the applied field varies sinusoidally at optical frequencies, the charged particles oscillate at the same frequency as the incident field. The oscillating dipoles in turn radiate into the medium and modify the way in which the wave propagates. Since the ion cores of the medium have much greater mass than the electrons, the motion of electrons becomes more significant for high

optical frequencies (ultraviolet and visible). For lower frequencies (infrared), the motions of the ions become more important, particularly, our main concern is the ionic lattice vibrations in solids.

The response of an ion to the optical electric field is that of a particle in an anharmonic potential well. The mechanical analogy of this is that the position of the particle in response to the optical field is governed by the equation of motion of an oscillator. The motion of charged particles in a medium can be considered linear with the applied field only if the displacement is small. However, for large distance,  $x$ , the restoring force is significantly nonlinear in  $x$ . The anharmonic response gives rise to an induced polarization which can be considered approximately linear or significantly nonlinear depending on the magnitude of the applied field. When the anharmonic terms are included, there is no longer an exact solution to the equation of motion.

The originator of the classical dipole oscillator model is Lorentz, so it is also called the Lorentz model. In this model, the light is treated as electromagnetic waves and the ions are treated as classical dipole oscillators. The forced damped cubic Duffing equation describes an oscillator with reduced mass  $M$  acting upon a nonlinear restoring force  $V(x)$  and a periodic external force  $q\mathbf{E}$  is described by the following equation of motion

$$M \frac{\partial^2 x}{\partial \mathbf{t}^2} + \Gamma_1 \frac{\partial x}{\partial \mathbf{t}} + \nabla V(x) = q\mathbf{E}_{loc} \quad (2.6)$$

In the former equation,  $x(\mathbf{t})$  is the displacement of the ions from its equilibrium position and  $q$  is the effective charge. The effective charge is usually smaller than

the charge on the electron because the transfer of the electron in the alkali halides for example from the alkali atom to the halogen atom is not complete. The cubic Duffing oscillator describes the motion of a classical particle in a double well potential  $V(x) = \frac{1}{2}\lambda_1 x^2 + \frac{1}{4}\lambda_2 x^4$  with  $\lambda_1$  and  $\lambda_2$  being the linear and the nonlinear spring constant respectively. The one dimensional Duffing potential is the simplest binding potential which may lead to a bistable response. Therefore;

$$M \frac{\partial^2 x}{\partial \mathbf{t}^2} + \Gamma_1 \frac{\partial x}{\partial \mathbf{t}} + \lambda_1 x + \lambda_2 x^3 = q\mathbf{E}_{loc} \quad (2.7)$$

Application of external field results in the rotation of these randomly oriented dipoles to align with the direction of the field  $\mathbf{p} = -qx(\mathbf{z})$ . In a small volume (but still have large number of dipoles) all initially considered to be oscillating in phase, the magnitude of the initial macroscopic polarization is  $\mathbf{P} = N\mathbf{p}$  Where  $\mathbf{p}$  is the dipole moment and  $N$  is the dipole density (Number of dipoles per unit volume). Therefore, the nonlinear equation of motion for the macroscopic polarization

$$\frac{\partial^2 \mathbf{P}}{\partial \mathbf{t}^2} + \Gamma \frac{\partial \mathbf{P}}{\partial \mathbf{t}} + \omega_0^2 \mathbf{P} + b \mathbf{P}^3 = \gamma \mathbf{E}_{loc} \quad (2.8)$$

In the above,  $\omega_0^2 = \lambda_1/M$  is the resonance frequency,  $\gamma = Nq^2/M$  is the coupling constant,  $b = \lambda_2/M N^2 q^2$  is the basic nonlinear constant, and  $\Gamma = \Gamma_1/M$  is the damping parameters. In linear régime, to derive the linear dielectric constant from the above equation, we ignore the nonlinear term by setting the coefficient  $b$  to zero

$$\frac{\partial^2 \mathbf{P}}{\partial \mathbf{t}^2} + \Gamma \frac{\partial \mathbf{P}}{\partial \mathbf{t}} + \omega_0^2 \mathbf{P} = \gamma \mathbf{E}_{loc} \quad (2.9)$$

Consider the driving field and the polarization to be time-harmonic with  $\exp(-i\omega t)$  dependence. Therefore, the ionic polarization  $P_i$  may be written as;

$$P_i = \gamma E_{loc} / (\omega_0^2 - \omega^2 - i\omega\Gamma) \quad (2.10)$$

The frequency-dependence of the material response reflects the fact that a material's polarization does not respond instantaneously to an applied field, the response must always be “causal” (arising after the applied field). Now, recalling the basic definition for the electric displacement;

$$D = \epsilon_0 \epsilon_r(\omega) E = \epsilon_0 E + (P_i + P_e) \quad (2.11)$$

In the above equation,  $P_e$  accounts for the electronic polarization exists in the crystal due to the displacement of the electrons in the atomic shells from the positive ion cores. Substituting (2.10) into (2.11)

$$\epsilon(\omega) = \overbrace{1 + P_e / \epsilon_0 E_{loc}}^{\text{electronic}} + \overbrace{\left[ \gamma / \epsilon_0 (\omega_0^2 - \omega^2 - i\omega\Gamma) \right]}^{\text{ionic}} \quad (2.12)$$

For  $\omega \ll \omega_0$ , both ionic and electronic contributes results in the familiar static dielectric constant  $\epsilon_r(0)$  (or simply  $\epsilon_s$ ). At the opposite end of the spectrum,  $\omega \gg \omega_0$ , the ionic contribution vanishes because the frequency there becomes too high for the ions to follow the oscillation of the field. In that range, the dielectric constant is denoted by  $\epsilon_r(\infty)$  (or simply  $\epsilon_\infty$ ) and contains only the electronic contribution. Therefore, the former equation may now be written as (Omar 1996)

$$\epsilon(\omega) = \epsilon_\infty + \left[ (\epsilon_s - \epsilon_\infty) \omega_T^2 / (\omega_T^2 - \omega^2 - i\omega\Gamma) \right] \quad (2.13)$$

In equation (2.13),  $\varepsilon(\omega)$  is written in terms of readily measured parameters. Table (2.1) shows these parameters for some ionic crystals.

**Table (2.1) Infrared lattice data for some ionic crystals (Omar 1996).**

Symbol	$\varepsilon_r(0)$	$\varepsilon_r(\infty)$	$\omega_T, 10^{13}$ rad/s	$\omega_L, 10^{13}$ rad/s	$q^*/q$
LiF	8.9	1.9	5.8	12	0.87
NaF	5.3	1.75	4.4	7.8	0.93
NaCl	5.62	2.25	3.08	5	0.74
NaBr	5.99	2.62	2.55	3.9	0.69
KBr	4.78	2.33	2.18	-	0.76
AgCl	12.3	4.04	1.94	3.4	0.78

We also note that, the resonance frequency  $\omega_0$  is related to the transverse optical frequency  $\omega_T$  through the linear relation (Ashcroft 1976 )

$$\omega_0^2 = [\varepsilon_s + 2/\varepsilon_\infty + 2]\omega_T^2 \quad (2.14)$$

Equation (2.12) may also be written in alternative form in terms of the plasma frequency  $\omega_p^2 = Nq^2/M\varepsilon_0$  (Bohren 1998);

$$\varepsilon(\omega) = \varepsilon_\infty + \left[ \frac{\omega_p^2}{(\omega_0^2 - \omega^2 - i\omega\Gamma)} \right] \quad (2.15)$$

Equation (2.15) may be written in the form  $\varepsilon(\omega) = \varepsilon'(\omega) + i\varepsilon''(\omega)$  where the real and imaginary parts are.

$$\varepsilon'(\omega) = \varepsilon_\infty + \frac{\omega_p^2 (\omega_0 - \omega)}{2\omega_0 \left[ (\omega_0 - \omega)^2 + (\Gamma/2)^2 \right]} \quad (2.16)$$

$$\varepsilon''(\omega) \simeq \frac{\Gamma \omega_p^2}{4\omega_0 \left[ (\omega_0 - \omega)^2 + (\Gamma/2)^2 \right]} \quad (2.17)$$

The above process of separating the dielectric constant  $\varepsilon(\omega)$  to its real and imaginary parts has its importance to estimate the damping parameter  $\Gamma$  (Bohren 1998). From (2.17), the maximum value of  $\varepsilon''$  at  $\omega = \omega_0$  is approximately  $\omega_p^2/\Gamma\omega_0$ . The width of the bell-shaped curve of  $\varepsilon''$  is  $\Gamma$  i.e.  $\varepsilon''$  falls one-half its maximum value when

$$(\omega_0 - \omega \approx \pm\Gamma/2) \quad (2.18)$$

Setting the Derivative of (1.16) with respect to  $(\omega_0 - \omega)$  equal to zero, therefore,  $\varepsilon'_{\max} = 1 + \varepsilon''_{\max}/2$  and  $\varepsilon'_{\min} = 1 - \varepsilon''_{\max}/2$  occurs at  $\omega_0 - \omega = +\Gamma/2$  and  $\omega_0 - \omega = -\Gamma/2$  respectively. Because of the superposition principle for amplitudes in the harmonic approximation, the complex polarizability is an additive quantity. Therefore, the dielectric function for a collection of oscillator is just the sum over the various oscillators (Bohren 1998).

$$\varepsilon(\omega) = \varepsilon_\infty + \sum_j \left[ \frac{\omega_{p_j}^2}{\omega_0^2 - \omega^2 - i\omega\Gamma_j} \right] \quad (2.19)$$

The dielectric function may also be written in terms of refractive index  $\varepsilon(\omega) = \tilde{n}^2(\omega) = [n(\omega) - i\kappa(\omega)]^2 = [n^2 - \kappa^2] + 2in\kappa$  where  $\tilde{n}$  is the complex refractive index,  $n$  is the real refractive index, and  $\kappa$  is the extinction coefficient. For normal incidence, the reflectivity  $R$  of an optical medium may be written as

$$R = \left| \frac{(\tilde{n} - 1)}{(\tilde{n} + 1)} \right|^2 = \frac{[(n - 1)^2 + \kappa^2]}{[(n + 1)^2 + \kappa^2]} \quad (2.20)$$

Fig. 2.4 shows the linear frequency-dependent dielectric function  $\varepsilon(\omega) = \varepsilon'(\omega) + i\varepsilon''(\omega)$  versus frequency  $\omega$  based on multiple oscillator model. The dashed curve represents the real part  $\varepsilon'(\omega)$  while the solid curve represents the imaginary part  $\varepsilon''(\omega)$ . The parameters  $\omega_T$  and  $\omega_L$  is the transverse and longitudinal optical phonon frequencies respectively.  $\omega_L$  is the frequency where  $\varepsilon'(\omega)$  vanishes while  $\omega_T$  is the frequency where  $\varepsilon'(\omega) \rightarrow \infty$ . Thus the absorption and extinction coefficients have their maximum values at  $\omega_T$ . The phenomena of a strong infrared reflection and absorption by the lattice are sometimes called “reststrahlen”. An important feature of Fig. 2.4 that the real part  $\varepsilon'(\omega)$  of the dielectric function is negative in the frequency range  $\omega_T < \omega < \omega_L$ . This means that in the range  $\omega_T < \omega < \omega_L$ ,  $n = 0$  and  $\kappa \neq 0$  which shows that the reflectivity  $R = 1$ . Therefore, an incident wave with frequency in the range  $\omega_T < \omega < \omega_L$  does not propagate in the crystal and suffers a total reflection.

Fig. 2.5 illustrates the dependence of reflectance  $R$  on the frequency  $\omega$  for MgO as determined by (2.19) for a two oscillator model (solid line) in comparison to the experimental results (in circles) measured by Jasperse (1966). The round off edges in of the reflectance spectrum in Fig. 2.5 is due to the damping term in equation (2.19). Such damping may be due to any of the phonon-collision mechanism or loss of energy to the environment.

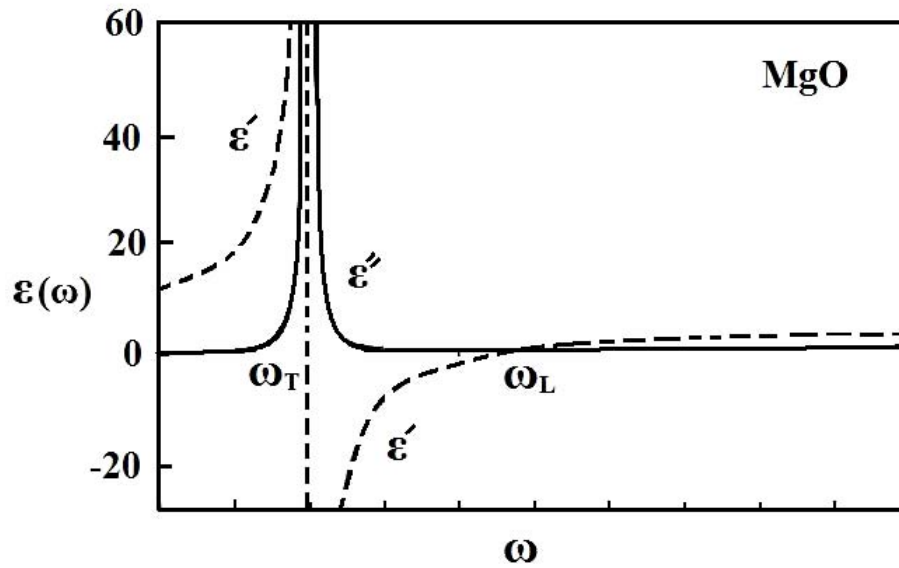


Figure 2.4 The linear frequency-dependent dielectric function  $\varepsilon(\omega) = \varepsilon'(\omega) + i\varepsilon''(\omega)$  versus frequency  $\omega$  for MgO. The dashed curve represents the real part  $\varepsilon'(\omega)$  while the solid curve represents the imaginary part  $\varepsilon''(\omega)$  (Jasperse 1966).

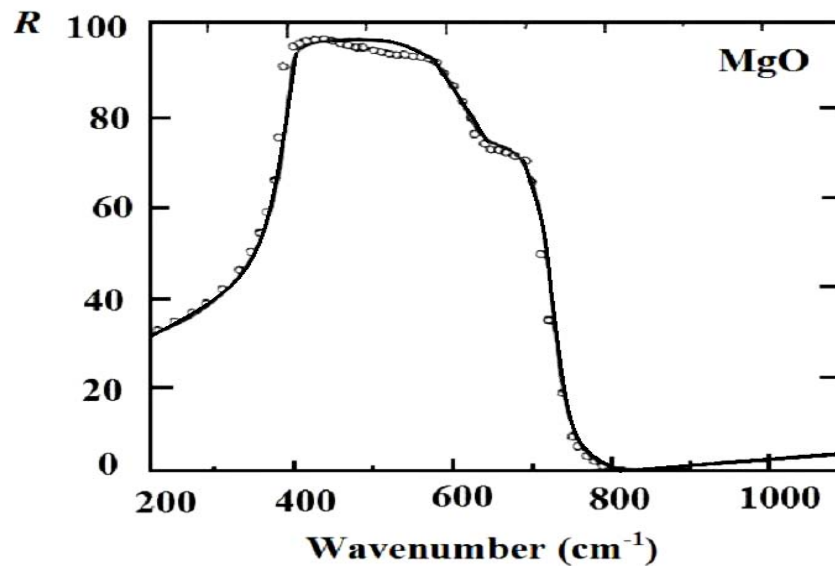


Figure 2.5 Reflectance  $R$  versus wavenumber; the solid line represents the theory, while the measurements (circles) are from Jasperse (1966).